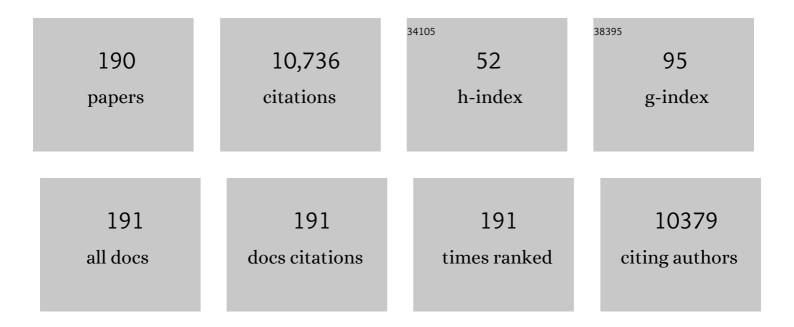
List of Publications by Year in descending order

Source: https://exaly.com/author-pdf/6620131/publications.pdf Version: 2024-02-01



#	Article	IF	CITATIONS
1	Polymer electrolytes for lithium polymer batteries. Journal of Materials Chemistry A, 2016, 4, 10038-10069.	10.3	1,048
2	The relationship between economic growth, energy consumption, and CO2 emissions: Empirical evidence from China. Science of the Total Environment, 2016, 542, 360-371.	8.0	441
3	Urbanization, economic growth, energy consumption, and CO2 emissions: Empirical evidence from countries with different income levels. Renewable and Sustainable Energy Reviews, 2018, 81, 2144-2159.	16.4	381
4	Urbanisation, energy consumption, and carbon dioxide emissions in China: A panel data analysis of China's provinces. Applied Energy, 2014, 136, 738-749.	10.1	371
5	Examining the impacts of socioeconomic factors, urban form, and transportation networks on CO2 emissions in China's megacities. Applied Energy, 2017, 185, 189-200.	10.1	306
6	The characteristics and drivers of fine particulate matter (PM2.5) distribution in China. Journal of Cleaner Production, 2017, 142, 1800-1809.	9.3	287
7	Changing urban forms and carbon dioxide emissions in China: A case study of 30 provincial capital cities. Applied Energy, 2015, 158, 519-531.	10.1	272
8	Quantifying the relationship between urban development intensity and carbon dioxide emissions using a panel data analysis. Ecological Indicators, 2015, 49, 121-131.	6.3	220
9	Spatiotemporal variations of energy-related CO 2 emissions in China and its influencing factors: An empirical analysis based on provincial panel data. Renewable and Sustainable Energy Reviews, 2016, 55, 505-515.	16.4	201
10	Preparation and properties of electrically conductive PPS/expanded graphite nanocomposites. Composites Science and Technology, 2007, 67, 2528-2534.	7.8	195
11	Examining the effects of socioeconomic development on fine particulate matter (PM2.5) in China's cities using spatial regression and the geographical detector technique. Science of the Total Environment, 2018, 619-620, 436-445.	8.0	189
12	Polymerâ€Based Solid Electrolytes: Material Selection, Design, and Application. Advanced Functional Materials, 2021, 31, 2007598.	14.9	164
13	Synthesis and properties of CO2-based plastics: Environmentally-friendly, energy-saving and biomedical polymeric materials. Progress in Polymer Science, 2018, 80, 163-182.	24.7	162
14	Sulfur-rich polymeric materials with semi-interpenetrating network structure as a novel lithium–sulfur cathode. Journal of Materials Chemistry A, 2014, 2, 9280.	10.3	149
15	A Rigid Naphthalenediimide Triangle for Organic Rechargeable Lithiumâ€ŀon Batteries. Advanced Materials, 2015, 27, 2907-2912.	21.0	145
16	Preparation and properties of sulfonated poly(fluorenyl ether ketone) membrane for vanadium redox flow battery application. Journal of Power Sources, 2010, 195, 2089-2095.	7.8	137
17	In Situ Preparation of Thin and Rigid COF Film on Li Anode as Artificial Solid Electrolyte Interphase Layer Resisting Li Dendrite Puncture. Advanced Functional Materials, 2020, 30, 1907717.	14.9	136
18	Novel Hierarchically Porous Carbon Materials Obtained from Natural Biopolymer as Host Matrixes for Lithium–Sulfur Battery Applications. ACS Applied Materials & Interfaces, 2014, 6, 13174-13182.	8.0	133

#	Article	IF	CITATIONS
19	Strategizing the relation between urbanization and air pollution: Empirical evidence from global countries. Journal of Cleaner Production, 2020, 243, 118615.	9.3	132
20	Effective Suppression of Lithium Dendrite Growth Using a Flexible Singleâ€lon Conducting Polymer Electrolyte. Small, 2018, 14, e1801420.	10.0	129
21	Highly effective synthesis of dimethyl carbonate from methanol and carbon dioxide using a novel copper–nickel/graphite bimetallic nanocomposite catalyst. Chemical Engineering Journal, 2009, 147, 287-296.	12.7	116
22	Completely biodegradable composites of poly(propylene carbonate) and short, lignocellulose fiberHildegardia populifolia. Journal of Polymer Science, Part B: Polymer Physics, 2004, 42, 666-675.	2.1	115
23	Synthesis and characterization of novel sulfonated poly(arylene thioether) ionomers for vanadiumredox flow battery applications. Energy and Environmental Science, 2010, 3, 622-628.	30.8	115
24	Synthesis and characterization of alternating copolymer from carbon dioxide and propylene oxide. Journal of Applied Polymer Science, 2002, 85, 2327-2334.	2.6	103
25	Polymers for high performance Li-S batteries: Material selection and structure design. Progress in Polymer Science, 2019, 89, 19-60.	24.7	103
26	Nearly 100% internal phosphorescence efficiency in a polymer light-emitting diode using a new iridium complex phosphor. Journal of Materials Chemistry, 2008, 18, 1636.	6.7	98
27	Synthesis and degradation behavior of poly(propylene carbonate) derived from carbon dioxide and propylene oxide. Journal of Applied Polymer Science, 2004, 92, 1840-1846.	2.6	89
28	TiO <sub>2</sub> -Doped CeO <sub>2</sub> Nanorod Catalyst for Direct Conversion of CO <sub>2</sub> and CH <sub>3</sub> OH to Dimethyl Carbonate: Catalytic Performance and Kinetic Study. ACS Omega, 2018, 3, 198-207.	3.5	89
29	Sulfur@graphene oxide core–shell particles as a rechargeable lithium–sulfur battery cathode material with high cycling stability and capacity. RSC Advances, 2013, 3, 4914.	3.6	88
30	Spatial differences and multi-mechanism of carbon footprint based on GWR model in provincial China. Journal of Chinese Geography, 2014, 24, 612-630.	3.9	84
31	Synthesis and Sulfonation of Poly(aryl ethers) Containing Triphenyl Methane and Tetraphenyl Methane Moieties from Isocynate-Masked Bisphenols. Macromolecules, 2004, 37, 3151-3158.	4.8	83
32	Mesoporous carbon materials prepared from litchi shell as sulfur encapsulator for lithium-sulfur battery application. Journal of Power Sources, 2016, 324, 547-555.	7.8	83
33	Sulfonated poly (fluorenyl ether ketone) membrane with embedded silica rich layer and enhanced proton selectivity for vanadium redox flow battery. Journal of Power Sources, 2010, 195, 7701-7708.	7.8	82
34	Catalytic materials for direct synthesis of dimethyl carbonate (DMC) from CO2. Journal of Cleaner Production, 2021, 279, 123344.	9.3	81
35	A Novel Single-Ion-Conducting Polymer Electrolyte Derived from CO <sub>2</sub> -Based Multifunctional Polycarbonate. ACS Applied Materials & Interfaces, 2016, 8, 33642-33648.	8.0	80
36	Sulfonated poly(fluorenyl ether ketone) membrane prepared via direct polymerization for PEM fuel cell application. Journal of Membrane Science, 2006, 280, 433-441.	8.2	76

#	Article	IF	CITATIONS
37	Synthesis and properties of novel sulfonated poly(arylene ether sulfone) ionomers for vanadium redox flow battery. Energy Conversion and Management, 2010, 51, 2816-2824.	9.2	75
38	Examining the spatially varying effects of factors on PM2.5 concentrations in Chinese cities using geographically weighted regression modeling. Environmental Pollution, 2019, 248, 792-803.	7.5	70
39	Examining the Impacts of Urban Form on Air Pollution in Developing Countries: A Case Study of China's Megacities. International Journal of Environmental Research and Public Health, 2018, 15, 1565.	2.6	68
40	Direct synthesis of dimethyl carbonate from carbon dioxide and methanol using supported copper (Ni,) Tj ETQqC	0 0 rgBT	Overlock 10
41	Direct synthesis of DMC from CH3OH and CO2 over V-doped Cu–Ni/AC catalysts. Catalysis Communications, 2009, 10, 1142-1145.	3.3	66
42	Nonstrained Î <sup>3</sup> -Butyrolactone to High-Molecular-Weight Poly(Î <sup>3</sup> -butyrolactone): Facile Bulk Polymerization Using Economical Ureas/Alkoxides. Macromolecules, 2018, 51, 9317-9322.	4.8	66
43	Single-ion conducting artificial solid electrolyte interphase layers for dendrite-free and highly stable lithium metal anodes. Journal of Materials Chemistry A, 2019, 7, 13113-13119.	10.3	66
44	Does modernization affect carbon dioxide emissions? A panel data analysis. Science of the Total Environment, 2019, 663, 426-435.	8.0	66
45	Comprehensive evaluation of safety performance and failure mechanism analysis for lithium sulfur pouch cells. Energy Storage Materials, 2020, 30, 87-97.	18.0	65
46	Highly safe lithium-ion batteries: High strength separator from polyformaldehyde/cellulose nanofibers blend. Journal of Power Sources, 2018, 400, 502-510.	7.8	64
47	Organic liquid electrolytes in Li-S batteries: actualities and perspectives. Energy Storage Materials, 2021, 34, 128-147.	18.0	63
48	Hierarchical Fe <sub>2</sub> 0 <sub>3</sub> @CNF fabric decorated with MoS <sub>2</sub> nanosheets as a robust anode for flexible lithium-ion batteries exhibiting ultrahigh areal capacity. Journal of Materials Chemistry A, 2018, 6, 16890-16899.	10.3	61
49	Fully alternating sustainable polyesters from epoxides and cyclic anhydrides: economical and metal-free dual catalysis. Green Chemistry, 2019, 21, 2469-2477.	9.0	61
50	Lithium (4-styrenesulfonyl) (trifluoromethanesulfonyl) imide based single-ion polymer electrolyte with superior battery performance. Energy Storage Materials, 2020, 24, 579-587.	18.0	61
51	Ultrastrong and Heat-Resistant Poly(ether ether ketone) Separator for Dendrite-Proof and Heat-Resistant Lithium-Ion Batteries. ACS Applied Energy Materials, 2019, 2, 3886-3895.	5.1	60
52	Network type sp3 boron-based single-ion conducting polymer electrolytes for lithium ion batteries. Journal of Power Sources, 2017, 360, 98-105.	7.8	59
53	Layer-by-layer self-assembly of PDDA/PSS-SPFEK composite membrane with low vanadium permeability for vanadium redox flow battery. RSC Advances, 2013, 3, 15467.	3.6	54
54	Effectively suppressing vanadium permeation in vanadium redox flow battery application with modified Nafion membrane with nacre-like nanoarchitectures. Journal of Power Sources, 2017, 352, 111-117.	7.8	54

#	Article	IF	CITATIONS
55	Strategies for inhibiting anode dendrite growth in lithium–sulfur batteries. Journal of Materials Chemistry A, 2020, 8, 4629-4646.	10.3	54
56	Novel Cu–Fe bimetal catalyst for the formation of dimethyl carbonate from carbon dioxide and methanol. RSC Advances, 2012, 2, 6831.	3.6	53
57	Dose urban landscape pattern affect CO2 emission efficiency? Empirical evidence from megacities in China. Journal of Cleaner Production, 2018, 203, 164-178.	9.3	53
58	Mechanism studies of terpolymerization of phthalic anhydride, propylene epoxide, and carbon dioxide catalyzed by ZnGA. RSC Advances, 2014, 4, 9503-9508.	3.6	52
59	Amphoteric ion exchange membrane synthesized by direct polymerization for vanadium redox flow battery application. International Journal of Hydrogen Energy, 2014, 39, 16123-16131.	7.1	51
60	Metal-Free Approach for a One-Pot Construction of Biodegradable Block Copolymers from Epoxides, Phthalic Anhydride, and CO <sub>2</sub> . ACS Sustainable Chemistry and Engineering, 2020, 8, 17860-17867.	6.7	51
61	Cerium oxide-based catalysts made by template-precipitation for the dimethyl carbonate synthesis from Carbon dioxide and methanol. Journal of Cleaner Production, 2015, 103, 847-853.	9.3	49
62	Preparation and properties of biodegradable blend containing poly (propylene carbonate) and starch acetate with different degrees of substitution. Carbohydrate Polymers, 2011, 86, 1260-1265.	10.2	48
63	Graphite oxide as a novel host material of catalytically active Cu–Ni bimetallic nanoparticles. Catalysis Communications, 2009, 10, 1529-1533.	3.3	46
64	Carbon felt interlayer derived from rice paper and its synergistic encapsulation of polysulfides for lithium-sulfur batteries. Applied Surface Science, 2018, 441, 914-922.	6.1	46
65	Specially designed carbon black nanoparticle-sulfur composite cathode materials with a novel structure for lithium–sulfur battery application. Journal of Power Sources, 2015, 285, 478-484.	7.8	45
66	CO <sub>2</sub> Nanoenrichment and Nanoconfinement in Cage of Imine Covalent Organic Frameworks for Highâ€Performance CO <sub>2</sub> Cathodes in Liâ€CO <sub>2</sub> Batteries. Small, 2019, 15, e1904830.	10.0	45
67	Layered zirconium phosphate sulfophenylphosphonates reinforced sulfonated poly (fluorenyl ether) Tj ETQq1 1 ( of Membrane Science, 2013, 443, 19-27.	).784314 ı 8.2	rgBT /Overloc 42
68	Electrostatic shield effect: an effective way to suppress dissolution of polysulfide anions in lithium–sulfur battery. Journal of Materials Chemistry A, 2014, 2, 15938-15944.	10.3	42
69	Porous composite membrane of PVDF/Sulfonic silica with high ion selectivity for vanadium redox flow battery. Journal of Membrane Science, 2019, 585, 230-237.	8.2	42
70	Synergetic Covalent and Spatial Confinement of Sulfur Species by Phthalazinone-Containing Covalent Triazine Frameworks for Ultrahigh Performance of Li–S Batteries. ACS Applied Materials & Interfaces, 2020, 12, 8296-8305.	8.0	42
71	Ultrahigh Li-ion conductive single-ion polymer electrolyte containing fluorinated polysulfonamide for quasi-solid-state Li-ion batteries. Journal of Materials Chemistry A, 2019, 7, 24251-24261.	10.3	41
72	Direct Synthesis of Dimethyl Carbonate from CO2 and CH3OH Using 0.4 nm Molecular Sieve Supported Cu-Ni Bimetal Catalyst. Chinese Journal of Chemical Engineering, 2012, 20, 906-913.	3.5	40

#	Article	IF	CITATIONS
73	A novel biodegradable polymeric surfactant synthesized from carbon dioxide, maleic anhydride and propylene epoxide. Polymer Chemistry, 2015, 6, 2076-2083.	3.9	40
74	Synthesis of sulfonated poly(fluorenyl ether thioether ketone)s with bulky-block structure and its application in vanadium redox flow battery. Polymer, 2011, 52, 5312-5319.	3.8	39
75	A proton exchange membrane fabricated from a chemically heterogeneous nonwoven with sandwich structure by the program-controlled co-electrospinning process. Chemical Communications, 2012, 48, 3415.	4.1	39
76	Novel polyaromatic ionomers with large hydrophilic domain and long hydrophobic chain targeting at highly proton conductive and stable membranes. Journal of Materials Chemistry, 2011, 21, 12068.	6.7	38
77	A Review on Sulfonated Polymer Composite/Organic-Inorganic Hybrid Membranes to Address Methanol Barrier Issue for Methanol Fuel Cells. Nanomaterials, 2019, 9, 668.	4.1	38
78	Design of dental implants at materials level: An overview. Journal of Biomedical Materials Research - Part A, 2020, 108, 1634-1661.	4.0	38
79	Pseudocapacitive Sodium Storage by Ferroelectric Sn <sub>2</sub> P <sub>2</sub> S <sub>6</sub> with Layered Nanostructure. Small, 2018, 14, e1704367.	10.0	37
80	Mechanical, Thermal, and Morphological Properties of Glass Fiber-reinforced Biodegradable Poly(propylene carbonate) Composites. Journal of Reinforced Plastics and Composites, 2010, 29, 1545-1550.	3.1	36
81	One-pot synthesis of terpolymers with long <scp>l</scp> -lactide rich sequence derived from propylene oxide, CO <sub>2</sub> , and <scp>l</scp> -lactide catalyzed by zinc adipate. Journal of Polymer Science Part A, 2015, 53, 1734-1741.	2.3	35
82	CO2 derived biodegradable polycarbonates: Synthesis, modification and applications. Advanced Industrial and Engineering Polymer Research, 2019, 2, 143-160.	4.7	32
83	Stable and ultrafast lithium storage for LiFePO4/C nanocomposites enabled by instantaneously carbonized acetylenic carbon-rich polymer. Carbon, 2019, 147, 19-26.	10.3	31
84	Macrodiols Derived from CO <sub>2</sub> -Based Polycarbonate as an Environmentally Friendly and Sustainable PVC Plasticizer: Effect of Hydrogen-Bond Formation. ACS Sustainable Chemistry and Engineering, 2018, 6, 8476-8484.	6.7	30
85	Cross-linkable and thermally stable aliphatic polycarbonates derived from CO2, propylene oxide and maleic anhydride. Journal of Polymer Research, 2009, 16, 91-97.	2.4	29
86	A highly efficient tris-cyclometalated iridium complex based on phenylphthalazine derivative for organic light-emitting diodes. Organic Electronics, 2009, 10, 618-622.	2.6	29
87	Synthesis, characterization and electroluminescence properties of iridium complexes based on pyridazine and phthalazine derivatives with C^NN structure. Synthetic Metals, 2010, 160, 2231-2238.	3.9	29
88	Multi-shell tin phosphide nanospheres as high performance anode material for a sodium ion battery. Sustainable Energy and Fuels, 2017, 1, 1944-1949.	4.9	29
89	One-Pot Synthesis of Dimethyl Hexane-1,6-diyldicarbamate from CO <sub>2</sub> , Methanol, and Diamine over CeO <sub>2</sub> Catalysts: A Route to an Isocyanate-Free Feedstock for Polyurethanes. ACS Sustainable Chemistry and Engineering, 2019, 7, 10708-10715.	6.7	29
90	Preparation and characterization of a novel layer-by-layer porous composite membrane for vanadium redox flow battery (VRB) applications. International Journal of Hydrogen Energy, 2014, 39, 16088-16095.	7.1	28

#	Article	IF	CITATIONS
91	Semi-crystalline terpolymers with varying chain sequence structures derived from CO <sub>2</sub> , cyclohexene oxide and ε-caprolactone: one-step synthesis catalyzed by tri-zinc complexes. Polymer Chemistry, 2015, 6, 1533-1540.	3.9	28
92	Interphase Building of Organic–Inorganic Hybrid Polymer Solid Electrolyte with Uniform Intermolecular Li <sup>+</sup> Path for Stable Lithium Metal Batteries. Small, 2021, 17, e2102454.	10.0	28
93	Polybenzimidazole-Based Semi-Interpenetrating Proton Exchange Membrane with Enhanced Stability and Excellent Performance for High-Temperature Proton Exchange Membrane Fuel Cells. ACS Applied Energy Materials, 2021, 4, 13316-13326.	5.1	28
94	Poly(Arylene Ether)s with Sulfonic Acid Groups on the Backbone and Pendant for Proton Exchange Membranes Used in PEMFC Applications. Fuel Cells, 2007, 7, 232-237.	2.4	27
95	Novel luminescent lanthanide complexes covalently linked to a terpyridine-functionalized silica network. Journal of Photochemistry and Photobiology A: Chemistry, 2007, 191, 74-79.	3.9	27
96	Thermal runaway features of lithium sulfur pouch cells at various states of charge evaluated by extended volume-accelerating rate calorimetry. Journal of Power Sources, 2021, 489, 229503.	7.8	27
97	Thermal degradation of poly(lactide-co-propylene carbonate) measured by TG/FTIR and Py-GC/MS. Polymer Degradation and Stability, 2015, 117, 16-21.	5.8	26
98	Instantaneous carbonization of an acetylenic polymer into highly conductive graphene-like carbon and its application in lithium–sulfur batteries. Journal of Materials Chemistry A, 2017, 5, 7015-7025.	10.3	26
99	Edge sulfurized graphene nanoplatelets via vacuum mechano-chemical reaction for lithium–sulfur batteries. Journal of Energy Chemistry, 2017, 26, 522-529.	12.9	26
100	A phosphonated phenol-formaldehyde-based high-temperature proton exchange membrane with intrinsic protonic conductors and proton transport channels. Journal of Materials Chemistry A, 2022, 10, 10916-10925.	10.3	26
101	Formation of Dimethyl Carbonate on Nature Clay Supported Bimetallic Copper-Nickel Catalysts. Journal of Cleaner Production, 2015, 103, 925-933.	9.3	25
102	Nonisocyanate CO <sub>2</sub> -Based Poly(ester- <i>co</i> -urethane)s with Tunable Performances: A Potential Alternative to Improve the Biodegradability of PBAT. ACS Sustainable Chemistry and Engineering, 2020, 8, 1923-1932.	6.7	25
103	Design and structure of catalysts: syntheses of carbon dioxide-based copolymers with cyclic anhydrides and/or cyclic esters. Polymer Journal, 2021, 53, 3-27.	2.7	25
104	Surface Reduced CeO2 Nanowires for Direct Conversion of CO2 and Methanol to Dimethyl Carbonate: Catalytic Performance and Role of Oxygen Vacancy. Catalysts, 2018, 8, 164.	3.5	24
105	Lithium Borate Containing Bifunctional Binder To Address Both Ion Transporting and Polysulfide Trapping for High-Performance Li–S Batteries. ACS Applied Materials & Interfaces, 2019, 11, 28968-28977.	8.0	24
106	Foldable and High Sulfur Loading 3D Carbon Electrode for High-performance Li-S Battery Application. Scientific Reports, 2016, 6, 33871.	3.3	23
107	Synthesis of Aliphatic Carbonate Macrodiols and Their Application as Sustainable Feedstock for Polyurethane. ACS Omega, 2017, 2, 3205-3213.	3.5	23
108	In Situ Laminated Separator Using Nitrogen–Sulfur Codoped Two-Dimensional Carbon Material to Anchor Polysulfides for High-Performance Li–S Batteries. ACS Applied Nano Materials, 2018, 1, 3807-3816.	5.0	23

#	Article	IF	CITATIONS
109	Covalent Organic Frameworks with Low Surface Work Function Enabled Stable Lithium Anode. Small, 2021, 17, e2101496.	10.0	23
110	Performance tailorable terpolymers synthesized from carbon dioxide, phthalic anhydride and propylene oxide using Lewis acid-base dual catalysts. Journal of CO2 Utilization, 2021, 49, 101558.	6.8	23
111	Highly effective direct synthesis of DMC from CH3OH and CO2 using novel Cu–Ni/C bimetallic composite catalysts. Chinese Chemical Letters, 2009, 20, 352-355.	9.0	22
112	Directly fluorinated polyaromatic composite membranes for vanadium redox flow batteries. Journal of Membrane Science, 2012, 415-416, 139-144.	8.2	22
113	Ring-opening polymerization of l-lactide and ε-caprolactone catalyzed by versatile tri-zinc complex: Synthesis of biodegradable polyester with gradient sequence structure. European Polymer Journal, 2016, 74, 109-119.	5.4	22
114	Addressing interface elimination: Boosting comprehensive performance of all-solid-state Li-S battery. Energy Storage Materials, 2021, 41, 563-570.	18.0	22
115	Synthesis and characterization of quaternary ammonium functionalized fluorene-containing cardo polymers for potential anion exchange membrane water electrolyzer applications. International Journal of Hydrogen Energy, 2012, 37, 16168-16176.	7.1	21
116	Zinc adipate/tertiary amine catalytic system: efficient synthesis of high molecular weight poly(propylene carbonate). Journal of Polymer Research, 2013, 20, 1.	2.4	21
117	Activities comparison of Schiff base zinc and tri-zinc complexes for alternating copolymerization of CO2 and epoxides. Polymer Chemistry, 2014, 5, 3838.	3.9	21
118	A Functional Separator Coated with Sulfonated Poly(Styrene-ethylene-butylene-styrene) to Synergistically Enhance the Electrochemical Performance and Anti-Self-Discharge Behavior of Li–S Batteries. ACS Applied Energy Materials, 2018, 1, 2555-2564.	5.1	21
119	Aqueous sodium alginate as binder: Dramatically improving the performance of dilithium terephthalate-based organic lithium ion batteries. Journal of Power Sources, 2019, 438, 227007.	7.8	21
120	Transparency Change Mechanochromism Based on a Robust PDMSâ€Hydrogel Bilayer Structure. Macromolecular Rapid Communications, 2021, 42, e2000446.	3.9	21
121	Transparent and super-gas-barrier PET film with surface coated by a polyelectrolyte and Borax. Polymer Journal, 2018, 50, 239-250.	2.7	20
122	Synthesis of Polylactide Nanocomposites Using an α-Zirconium Phosphate Nanosheet-Supported Zinc Catalyst via in Situ Polymerization. ACS Applied Polymer Materials, 2019, 1, 1382-1389.	4.4	20
123	Spatial Heterogeneity in the Determinants of Urban Form: An Analysis of Chinese Cities with a GWR Approach. Sustainability, 2019, 11, 479.	3.2	20
124	Near-infrared luminescent lanthanide (Er, Nd) complexes covalently bonded to a terpyridine-functionalized silica matrix. Photochemical and Photobiological Sciences, 2007, 6, 519.	2.9	19
125	Foaming and chain extension of completely biodegradable poly(propylene carbonate) using DPT as blowing agent. Journal of Polymer Research, 2007, 14, 245-251.	2.4	19
126	Biodegradable and Toughened Composite of Poly(Propylene Carbonate)/Thermoplastic Polyurethane (PPC/TPU): Effect of Hydrogen Bonding. International Journal of Molecular Sciences, 2018, 19, 2032.	4.1	19

#	Article	IF	CITATIONS
127	A Highly Immobilized Organic Anode Material for High Performance Rechargeable Lithium Batteries. ACS Applied Materials & Interfaces, 2020, 12, 36237-36246.	8.0	19
128	Gradient terpolymers with long ε-caprolactone rich sequence derived from propylene oxide, CO2, and ε-caprolactone catalyzed by zinc glutarate. European Polymer Journal, 2016, 84, 245-255.	5.4	18
129	Toward Theoretically Cycling-Stable Lithium–Sulfur Battery Using a Foldable and Compositionally Heterogeneous Cathode. ACS Applied Materials & Interfaces, 2017, 9, 43640-43647.	8.0	18
130	Polyphenylene Sulfide Separator for High Safety Lithium-Ion Batteries. Journal of the Electrochemical Society, 2019, 166, A1644-A1652.	2.9	18
131	Artificial Single-Ion Conducting Polymer Solid Electrolyte Interphase Layer toward Highly Stable Lithium Anode. ACS Applied Energy Materials, 2021, 4, 862-869.	5.1	18
132	Polysulfide rubber-based sulfur-rich composites as cathode material for high energy lithium/sulfur batteries. International Journal of Hydrogen Energy, 2014, 39, 16067-16072.	7.1	16
133	Hierarchical NiCoP/C Hollow Nanoflowers for Enhanced Lithium Storage. ACS Applied Nano Materials, 2019, 2, 6880-6888.	5.0	16
134	Heteropolyacid Salt Catalysts for Methanol Conversion to Hydrocarbons and Dimethyl Ether: Effect of Reaction Temperature. Catalysts, 2019, 9, 320.	3.5	16
135	Miscibility, properties and morphology of biodegradable blends of UHMW-PPC/PVA/EVOH. Journal of Polymer Research, 2011, 18, 715-720.	2.4	15
136	Copolymerization of propylene oxide and carbon dioxide in the presence of diphenylmethane diisoyanate. Journal of Polymer Research, 2011, 18, 1479-1486.	2.4	15
137	Biodegradable PPC/(PVA-TPU) ternary blend blown films with enhanced mechanical properties. Journal of Polymer Research, 2016, 23, 1.	2.4	15
138	Kinetic and mechanistic investigation for the copolymerization of CO <sub>2</sub> and cyclohexene oxide catalyzed by trizinc complexes. Polymer Chemistry, 2017, 8, 3632-3640.	3.9	15
139	Thermal degradation behavior of Copoly(propylene carbonate Îμ-caprolactone) investigated using TG/FTIR and Py-GC/MS methodologies. Polymer Testing, 2017, 58, 13-20.	4.8	15
140	High performance poly(urethane-co-amide) from CO2-based dicarbamate: an alternative to long chain polyamide. RSC Advances, 2019, 9, 26080-26090.	3.6	15
141	Sulfonated poly(fluorenyl ether ketone) ionomers containing aliphatic functional segments for fuel cell applications. International Journal of Hydrogen Energy, 2012, 37, 4553-4562.	7.1	14
142	Nano-Brick Wall Architectures Account for Super Oxygen Barrier PET Film by Quadlayer Assembly of Polyelectrolytes and α-ZrP Nanoplatelets. Polymers, 2018, 10, 1082.	4.5	14
143	Continuous Dimethyl Carbonate Synthesis from CO2 and Methanol Using Cu-Ni@VSiO as Catalyst Synthesized by a Novel Sulfuration Method. Catalysts, 2018, 8, 142.	3.5	14
144	Poly(propylene carbonate)/aluminum flake composite films with enhanced gas barrier properties. Journal of Applied Polymer Science, 2015, 132, .	2.6	13

#	Article	IF	CITATIONS
145	<i>In situ</i> template synthesis of hierarchical porous carbon used for high performance lithium–sulfur batteries. RSC Advances, 2018, 8, 4503-4513.	3.6	13
146	Effect of water management in membrane and cathode catalyst layers on suppressing the performance hysteresis phenomenon in anion-exchange membrane fuel cells. Journal of Power Sources, 2022, 522, 230997.	7.8	13
147	A rechargeable Li–CO <sub>2</sub> battery based on the preservation of dimethyl sulfoxide. Journal of Materials Chemistry A, 2022, 10, 13821-13828.	10.3	13
148	Electrochemical synthesis of dimethyl carbonate from CO2 and methanol over carbonaceous material supported DBU in a capacitor-like cell reactor. RSC Advances, 2016, 6, 40010-40016.	3.6	12
149	A Novel Multiblock Copolymer of CO <sub>2</sub> -Based PPC- <i>mb</i> -PBS: From Simulation to Experiment. ACS Sustainable Chemistry and Engineering, 2017, 5, 5922-5930.	6.7	12
150	Effect of Alkali-Doping on the Performance of Diatomite Supported Cu-Ni Bimetal Catalysts for Direct Synthesis of Dimethyl Carbonate. Catalysts, 2018, 8, 302.	3.5	12
151	Co-Ni Cyanide Bi-Metal Catalysts: Copolymerization of Carbon Dioxide with Propylene Oxide and Chain Transfer Agents. Catalysts, 2019, 9, 632.	3.5	12
152	A Robust Composite Proton Exchange Membrane of Sulfonated Poly (Fluorenyl Ether Ketone) with an Electrospun Polyimide Mat for Direct Methanol Fuel Cells Application. Polymers, 2021, 13, 523.	4.5	12
153	Semi-interpenetrating Network Membrane from Polyethyleneimine-Epoxy Resin and Polybenzimidazole for HT-PEM Fuel Cells. Advances in Polymer Technology, 2020, 2020, 1-8.	1.7	12
154	Novel ternary block copolymerization of carbon dioxide with cyclohexene oxide and propylene oxide using zinc complex catalyst. Journal of Polymer Research, 2012, 19, 1.	2.4	11
155	Structure properties of a highly luminescent yellow emitting material for OLED and its application. RSC Advances, 2013, 3, 215-220.	3.6	11
156	Effective suppression of lithium dendrite growth using fluorinated polysulfonamide-containing single-ion conducting polymer electrolytes. Materials Advances, 2020, 1, 873-879.	5.4	11
157	Fabrication and properties of degradable PPC/EVOH/starch/CaCO3 composites. Journal Wuhan University of Technology, Materials Science Edition, 2008, 23, 362-366.	1.0	10
158	Thermal degradation and isothermal crystalline behavior of poly(trimethylene terephthalate). Chinese Chemical Letters, 2009, 20, 487-491.	9.0	10
159	Surface Fluorination of Poly(fluorenyl ether ketone) Ionomers as Proton Exchange Membranes for Fuel Cell Application. Fuel Cells, 2011, 11, 353-360.	2.4	10
160	Synthesis of Co <sub>1.5</sub> PW <sub>12</sub> O <sub>40</sub> and its catalytic performance of completely converting methanol to ethylene. Chemical Communications, 2016, 52, 1151-1153.	4.1	10
161	Performance Enhanced SAPO-34 Catalyst for Methanol to Olefins: Template Synthesis Using a CO2-Based Polyurea. Catalysts, 2019, 9, 16.	3.5	10
162	3D Network Structural Poly (Aryl Ether Ketone)-Polybenzimidazole Polymer for High-Temperature Proton Exchange Membrane Fuel Cells. Advances in Polymer Technology, 2020, 2020, 1-13.	1.7	10

#	Article	IF	CITATIONS
163	Biodegradable Copolymers from CO <sub>2</sub> , Epoxides, and Anhydrides Catalyzed by Organoborane/Tertiary Amine Pairs: High Selectivity and Productivity. Macromolecules, 2022, 55, 6120-6130.	4.8	10
164	Porous Diatomite-Immobilized Cu–Ni Bimetallic Nanocatalysts for Direct Synthesis of Dimethyl Carbonate. Journal of Nanomaterials, 2012, 2012, 1-8.	2.7	9
165	A novel lithium–sulfur battery cathode from butadiene rubber-caged sulfur-rich polymeric composites. RSC Advances, 2015, 5, 38792-38800.	3.6	9
166	Nonisothermal crystallization behavior and kinetics of poly(l-lactide-co-propylene carbonate). Journal of Thermal Analysis and Calorimetry, 2015, 121, 877-883.	3.6	8
167	Enhanced Properties of Biodegradable Poly(Propylene Carbonate)/Polyvinyl Formal Blends by Melting Compounding. Polymers, 2018, 10, 771.	4.5	8
168	ls superparelectric 2-dimensional Sn2P2S6 having a "higher dielectric constant―desirable for more real Na+ pseudocapacitance?. Nano Energy, 2019, 61, 462-470.	16.0	8
169	Multiblock copolymers of PPC with oligomeric PBS: with low brittle–toughness transition temperature. RSC Advances, 2018, 8, 14722-14731.	3.6	7
170	Crosslinked Polybenzimidazoles Containing Functional CrosslinkersAs High-Temperature Proton Exchange Membranes: Enhanced Strength and Conductivity. Journal of the Electrochemical Society, 2022, 169, 024502.	2.9	7
171	Polybenzimidazole Confined in Semi-Interpenetrating Networks of Crosslinked Poly (Arylene Ether) Tj ETQq1 1 0	.784314 r 4.1	gBŢ /Overloc
172	Ionically Crosslinked Composite Membranes from Polybenzimidazole and Sulfonated Poly (fluorenyl) Tj ETQqO O 114509.	0 rgBT /0 2.9	verlock 10 Tf 6
173	Effect of In-Situ Dehydration on Activity and Stability of Cu–Ni–K2O/Diatomite as Catalyst for Direct Synthesis of Dimethyl Carbonate. Catalysts, 2018, 8, 343.	3.5	5
174	Addressing Passivation of a Sulfur Electrode in Li–S Pouch Cells for Dramatically Improving Their Cyclic Stability. ACS Applied Materials & Interfaces, 2020, 12, 29296-29301.	8.0	5
175	Construction of KB@ZIF-8/PP Composite Separator for Lithium–Sulfur Batteries with Enhanced Electrochemical Performance. Polymers, 2021, 13, 4210.	4.5	5
176	2D NMR study on chemical structure of the co-oligomers from carbon dioxide/propylene oxide/diol synthesized by a metal-free catalyst. Polymer Testing, 2022, 107, 107485.	4.8	5
177	Syntheses, Structures and Proton Conductivities of Polyphthalazinone Ionomers Derived from a Direct NC Coupling Reaction. Macromolecular Chemistry and Physics, 2006, 207, 653-659.	2.2	4
178	Highly Active SO4 2â^'/xTiO2–ZrO2 Catalysts for the Esterification Between Terephthalic Acid and 1,3-Propanediol. Catalysis Letters, 2009, 131, 305-311.	2.6	4
179	A novel thermoplastic elastomer from double CO2-Route oligomers. Advanced Industrial and Engineering Polymer Research, 2019, 2, 186-195.	4.7	4
180	Low-Carbon and Nanosheathed ZnCo <sub>2</sub> O <sub>4</sub> Spheroids with Porous Architecture for Boosted Lithium Storage Properties. Research, 2019, 2019, 1354829.	5.7	4

#	Article	IF	CITATIONS
181	Both Phosphonic Acid- and Fluorine-Containing Poly(aryl ether)–hydroxyapatite Biocomposites: Toward Enhanced Biocompatibility and Bonelike Elastic Modulus. ACS Applied Bio Materials, 2020, 3, 9019-9030.	4.6	4
182	Correlation Between Crystallization Behavior and Mechanical Properties of Biodegradable Poly(Caprolactone- <i>co</i> -Cyclohexene Carbonate). Polymer-Plastics Technology and Engineering, 2018, 57, 1530-1541.	1.9	3
183	EFFECTS OF REACTION TIME AND PRESSURE ON THE COPOLYMERIZATION OF CARBON DIOXIDE AND PROPYLENE OXIDE USING SUPPORTED ZINC GLUTARATE CATALYST. Acta Polymerica Sinica, 2010, 010, 1148-1151.	0.0	3
184	Simulation of TSV Protrusion in 3DIC Integration by Directly Loading on Coarse-Grained Phase-Field Crystal Model. Electronics (Switzerland), 2022, 11, 221.	3.1	3
185	Excavating Anomalous Capacity Increase of Li–S Pouch Cells by Electrochemical Oscillation Formation. ACS Applied Materials & Interfaces, 2022, 14, 22197-22205.	8.0	2
186	Synthesis and properties of polycyclic phosphonate resins using one-pot method under ultrasound irradiation. Journal of Polymer Research, 2011, 18, 2351-2358.	2.4	1
187	Mechanical properties of block poly(propylene carbonateâ€cyclohexyl carbonate) investigated by nanoindentation and DMA methodologies. Journal of Applied Polymer Science, 2013, 128, 1979-1986.	2.6	1
188	Lithiumâ€Ion Batteries: A Rigid Naphthalenediimide Triangle for Organic Rechargeable Lithiumâ€Ion Batteries (Adv. Mater. 18/2015). Advanced Materials, 2015, 27, 2948-2948.	21.0	1
189	Advanced Technologies for Liquid–Redox Rechargeable Batteries. Electrochemical Energy Storage and Conversion, 2015, , 515-534.	0.0	0
190	A Novel Gel Polymer Electrolyte by Thiol-Ene Click Reaction Derived from CO2-Based Polycarbonate for Lithium-Ion Batteries. Advances in Polymer Technology, 2020, 2020, 1-12.	1.7	0